Journal of Sound and Vibration (2000) **229**(4), 1013–1022
doi:10.1006/jsvi.1999.2499, available online at http://www.idealibrary.com on IDEAL®

MODAL ACTUATORS AND SENSORS

W. GAWRONSKI

Jet Propulsion Laboratory, California Institute of Technology, Pasadena, CA 91109, *U.S.A.*

(*Received* 3 *December* 1998, *and in final form* 6 *July* 1999)

1. INTRODUCTION

The micromachining, nanofabrication, and distributed sensor/actuator technologies enable the implementation of large number of actuators and sensors on a flexible structure [1]. This massive instrumentation is a part of smart materials and of smart structures. For example, they are used for the active and passive structural vibration damping, active and passive noise damping and control, active shaping of surfaces of radiotelescopes and optical devices, health monitoring of structures, and shaping of aircraft surface for aerodynamic control. Using the large number of actuators and sensors requires special algorithms to determine their optimal locations. The definition of optimal location depends on application. Many techniques were proposed for the determination of the actuator and sensor locations, see for example references [2–11]. The application of the actuators and sensors can be extended if one allows for the variations not only of the actuators and sensors locations but also their gains.

In some structural tests it is desirable to isolate (i.e., excite and measure) a single mode. Such technique considerably simplifies the determination of modal parameters, see reference [12]. This was first achieved by using the force appropriation method, called also the Asher method, see reference [13], or phase separation method, see reference [14]. In this method a spatial distribution and the amplitudes of a harmonic input force are chosen to excite a single structural mode. A technique for the determination of the actuator/sensor locations and their gains, as presented in this paper, is based on the relationship between the modal and nodal co-ordinates of the actuator or sensor locations. As distinct from the force appropriation method it does not require the input force to be a harmonic one. Rather, it determines the actuator locations and actuator gains, while the input force time history is irrelevant (modal actuator acts as a filter). The locations and gains, for example, can be implemented as a width-shaped piezoelectric film. Finally, it allows for excitation and observation of not only a single structural mode but also of a set of selected modes, each one with the assigned amplitude. The presented method applies to both the actuators, and to the sensors. Such actuators or sensors are called modal actuators or sensors. Modal actuators or sensors in a different formulation were presented in references [15–17] with application to

0022-460X/00/041013 + 10 $35.00/0

structural acoustic problems. Modal actuator sensors in structural dynamics were investigated in references [2,18] using the state-space representation and the concept of the controllability and observability grammians. The presented method is illustrated with various modal actuators and sensors applied to a clamped beam.

2. MODAL MODEL

A structural model is characterized by its mass, stiffness, and damping matrices, as well as by the sensor and actuator locations. It is represented by the following second order differential equation:

$$M\ddot{q} + D\dot{q} + Kq = B_o u, \qquad y = C_{oq}q + C_{ov}\dot{q}. \tag{1}$$

In this equation q is the $n_d \times 1$ displacement vector, u is the $s \times 1$ input vector, y is the output vector, $r \times 1$, M is the mass matrix, $n_d \times n_d$, D is the damping matrix, $n_d \times n_d$, and K is the stiffness matrix, $n_d \times n_d$. The nodal input matrix B_o is $n_d \times s$, the nodal output displacement matrix C_{oq} is $r \times n_d$, and the nodal output velocity matrix C_{ov} is $r \times n_d$. The mass matrix is positive definite, and the stiffness and damping matrices are positive semidefinite. n_d is the number of dofs, s is the number of actuators, r is the number of sensors.

The above equation is also obtained in the modal co-ordinates using the modal transformation, derived as follows. For a small proportional damping let ω_i be the ith natural frequency and ϕ_i be the ith natural mode, or mode shape. Define the matrix of natural frequencies, $\Omega = \mathrm{diag}(\omega_1, \omega_2, \ldots, \omega_n)$, and the modal matrix Φ, $n_d \times n$, $\Phi = [\phi_1 \quad \phi_2 \quad \cdots \quad \phi_n]$, which consists of n natural modes of a structure. It transforms the mass and stiffness matrices into the modal mass matrix $M_m = \Phi^T M \Phi$, and the modal stiffness matrix $K_m = \Phi^T K \Phi$. Both matrices are diagonal. Proportional damping matrix can be diagonalized as well, obtaining the modal damping matrix $D_m = \Phi^T D \Phi$.

A new variable, q_m, called the modal displacement vector is introduced, such that $q = \Phi q_m$. Pre-multiplying equation (1) by Φ^T, and subsequently by M_m^{-1} gives the modal model

$$\ddot{q}_m + 2Z\Omega\dot{q}_m + \Omega^2 q_m = B_m u, \qquad y = C_{mq}q_m + C_{mv}\dot{q}_m, \tag{2}$$

where $\Omega = M_m^{-1/2}K_m^{1/2}$ is the matrix of natural frequencies, $Z = 0{\cdot}5M_m^{-1}D_m\Omega^{-1}$ is a diagonal matrix of the modal damping ratios, and B_m is the modal input matrix

$$B_m = M_m^{-1}\Phi^T B_o, \tag{3}$$

while C_{mq} and C_{mv} are the modal displacement and rate matrices respectively:

$$C_{mq} = C_{oq}\Phi, \qquad C_{mv} = C_{ov}\Phi. \tag{4}$$

The modal equation (2) can be written also as a set of n independent equations for each modal displacement:

$$\ddot{q}_{mi} + 2\zeta_i \omega_i \dot{q}_{mi} + \omega_i^2 q_{mi} = b_{mi} u, \qquad y_i = c_{mqi} q_{mi} + c_{mvi} \dot{q}_{mi}, \quad i = 1, \ldots, n. \tag{5}$$

In the above equations, y_i is the system output due to the ith mode dynamics, such that $y = \sum_{i=1}^{n} y_i$, while b_{mi} is the ith row of B_m, and c_{mqi} and c_{mvi} are the ith columns of C_{mq}, and C_{mv} respectively.

3. MODAL ACTUATORS

The task is to determine the locations and gains of the actuators such that n_m modes of the system are excited with approximately the same amplitude, where $1 \leqslant n_m \leqslant n$, and n is the total number of considered modes. Note that if the ith mode is not excited the corresponding ith row, b_{mi}, of the modal input matrix, B_m, is zero. Thus, assigning entries of b_{mi} either 1 or 0, one makes the ith mode excited or not. This assigned input matrix we denote B_m. For example, if one wants to excite the first mode only, B_m is a one-column matrix of a form $B_{ms} = [1 \quad 0 \quad \cdots \quad 0]^T$. On the other hand, if one wants to excite all modes independently and equally, one assigns a unit matrix, $B_m = I$.

Given (or assigned) the modal matrix B_m the nodal matrix B_o is derived from equation (3). Equation (3) can be re-written as

$$B_m = R B_o, \tag{6}$$

where $R = M_m^{-1} \Phi^T$. Matrix R is of dimensions $n \times n_d$. Recall that the number of assigned modes is $n_m \leqslant n$. If the assigned modes are controllable, i.e., the rank of R is n_m, the least-square solution of equation (6) is

$$B_o = R^+ B_m. \tag{7}$$

In the above equation, R^+ is pseudoinverse of R, $R^+ = V \Sigma^{-1} U^T$, where U, Σ, and V are obtained from the singular value decomposition of R, i.e., $R = U \Sigma V^T$.

3.1. EXAMPLE 1

Consider a clamped beam of 150 cm length, cross-section of 1 cm^2, divided into 15 equal elements, as in Figure 1, where the filled nodes 1 and 16 are the clamped ones. The vertical displacement sensors are located at nodes 2–15, and the single output is the sum of the sensor readings. Actuator locations shall be determined such that the second mode with 0·01 modal gain is excited, and the remaining modes are not excited. The first nine modes are considered.

The assigned modal matrix is in this case $B_m^T = [0 \;\; 0{\cdot}01 \;\; 0 \;\; 0 \;\; 0 \;\; 0 \;\; 0 \;\; 0 \;\; 0]^T$. From equation (7), for this modal input matrix, a nodal input matrix B_o is determined. It

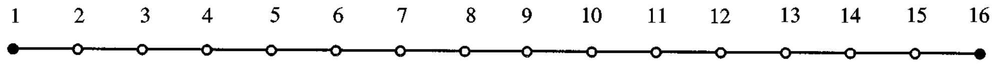

Figure 1. A clamped beam.

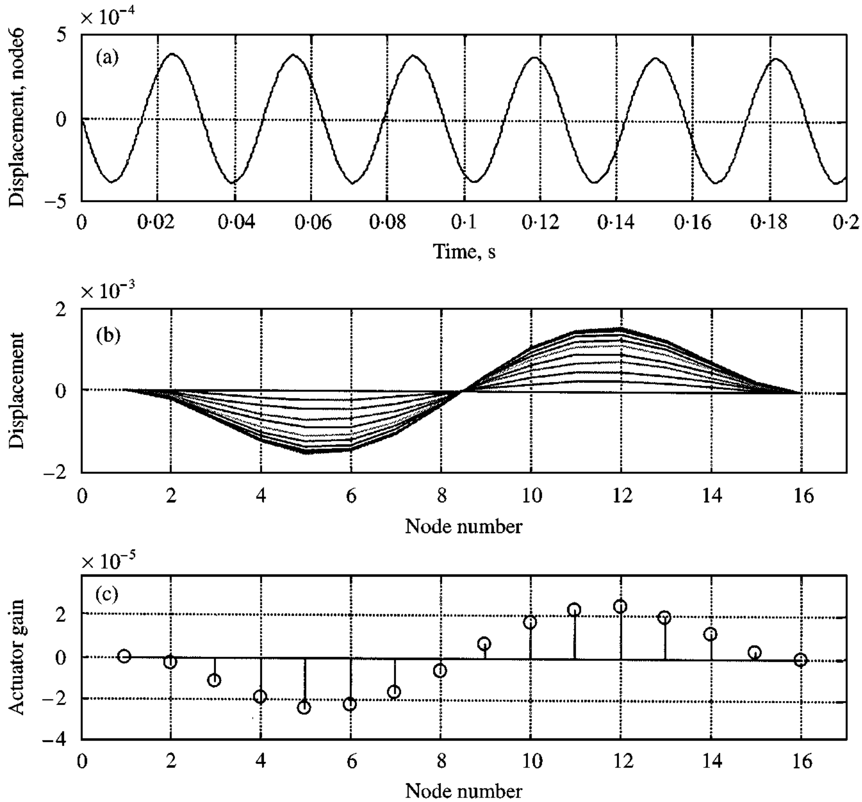

Figure 2. Beam with the second-mode modal actuator: (a) impulse response at node 6, (b) nodal displacements for the first 10 time samples, and (c) actuator gains.

contains gains for the vertical forces at the nodes 2–15. The gain distribution of the actuators is shown in Figure 2(c). Note that this distribution is proportional to the second mode shape. This distribution can be implemented as a piezoelectric actuator. Consider a case when the gain of the piezoelectric actuator is proportional to its width. Thus, the shape of a hypothetical piezoelectric actuator that excites the second mode is shown in Figure 3.

For the input and the outputs defined as above the magnitude of the transfer function is presented in Figure 4. The plot shows clearly that only the second mode is excited. This is confirmed with the impulse response at node 6, Figure 2(a), where only second harmonic is excited. Figure 2(b) shows the simultaneous displacement of nodes 1–16 for the first 10 time samples. They also confirm that only the second mode shape was excited.

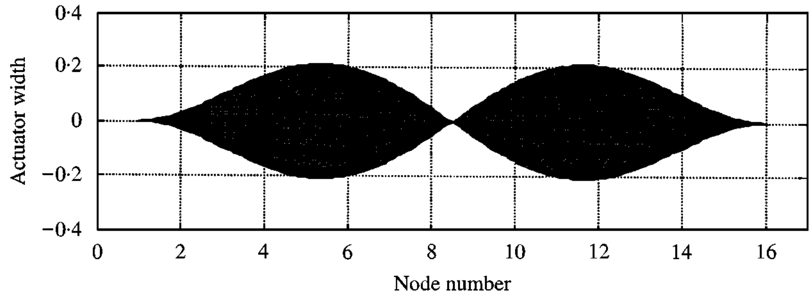

Figure 3. Piezoelectric actuator width that excites the second mode.

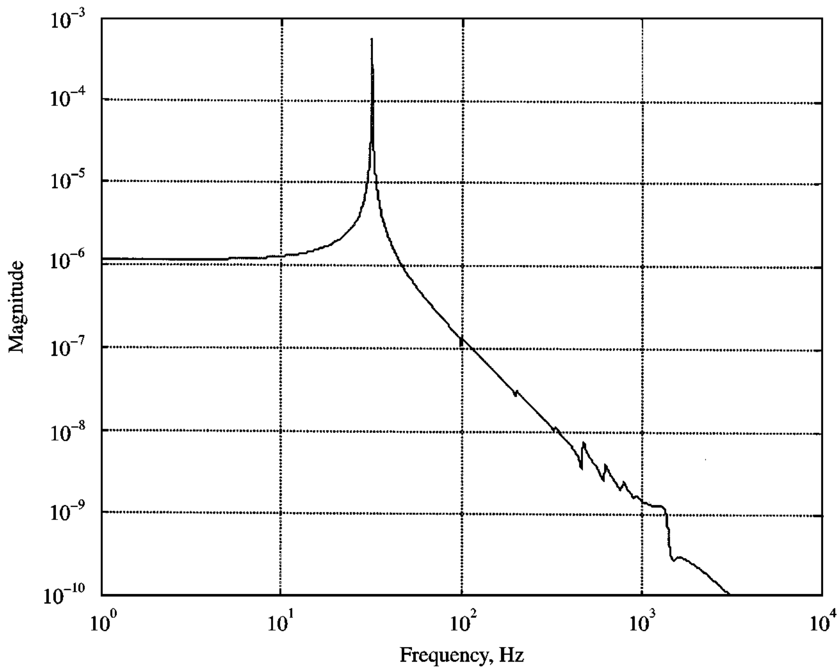

Figure 4. Magnitude of a transfer function with the second-mode modal actuator.

If one wants to excite a mode with a certain amplitude, one needs to scale (or weight) properly the input matrix B_m. The H_∞ norm is used as a measure of the amplitude of the ith mode. In case of a single-input–single-output system the H_∞ norm of the ith mode is equal to the height of the ith resonance peak. In case of multiple inputs (or outputs) the H_∞ norm of the ith mode is approximately equal to the root-mean-square sum of the ith resonance peaks corresponding to each input (or output), see reference [2]. It is approximately determined as [2]

$$\|G_i\|_\infty \cong \frac{\|b_{mi}\|_2 \|c_{mi}\|_2}{2\zeta_i \omega_i}, \tag{8}$$

where $\|\cdot\|_2$ denotes the Euclidean norm, and $\|b_{mi}\|_2$, $\|c_{mi}\|_2$ are called the actuator and sensor gains respectively. Thus, the required actuator gain $\|b_{mi}\|_2$ that results in the assigned resonance amplitude $\|G_i\|_\infty$ is obtained as $\|b_{mi}\|_2 \cong 2\zeta_i\omega_i\|G_i\|_\infty/\|c_{mi}\|_2$, hence the ith mode has to be weighted with

$$w_i = \frac{2\zeta_i\omega_i\|G_i\|_\infty}{\|c_{mi}\|_2}. \tag{9}$$

Define the weight matrix $W = \mathrm{diag}(w_1, w_2, \ldots, w_n)$, then the specified matrix that sets the required output modal amplitudes is

$$B_{mw} = WB_m. \tag{10}$$

3.2. EXAMPLE 2

The same beam is considered. All nine modes need to be excited by a single actuator with the amplitude of 0·01. Therefore, the assigned matrix B_m is $B_m^T = 0{\cdot}01 \times [1 \quad 1 \quad 1 \quad 1 \quad 1 \quad 1 \quad 1 \quad 1 \quad 1]^T$, and the weighting matrix is obtained from equation (9). The resulting gains of the nodal input matrix B_o shown in Figure 5(c)

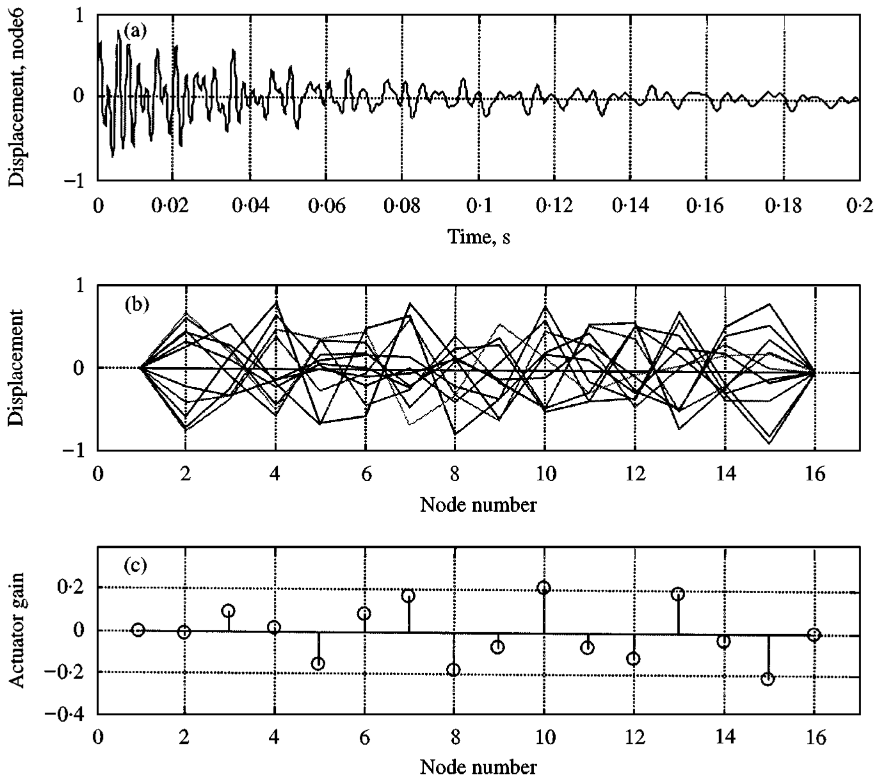

Figure 5. The beam with the nine-mode modal actuator: (a) impulse response at node 6, (b) nodal displacements for the first 10 time samples, and (c) actuator gains.

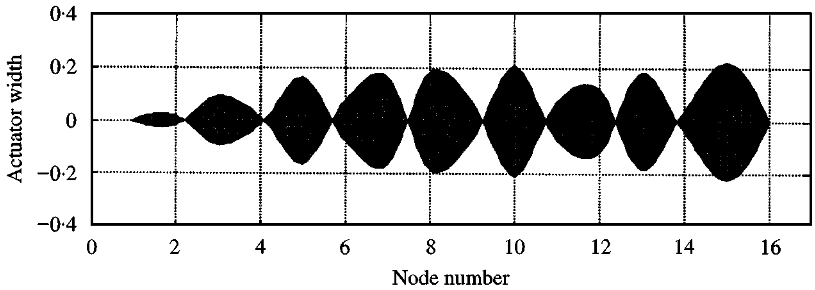

Figure 6. Piezoelectric actuator width that excites all nine modes.

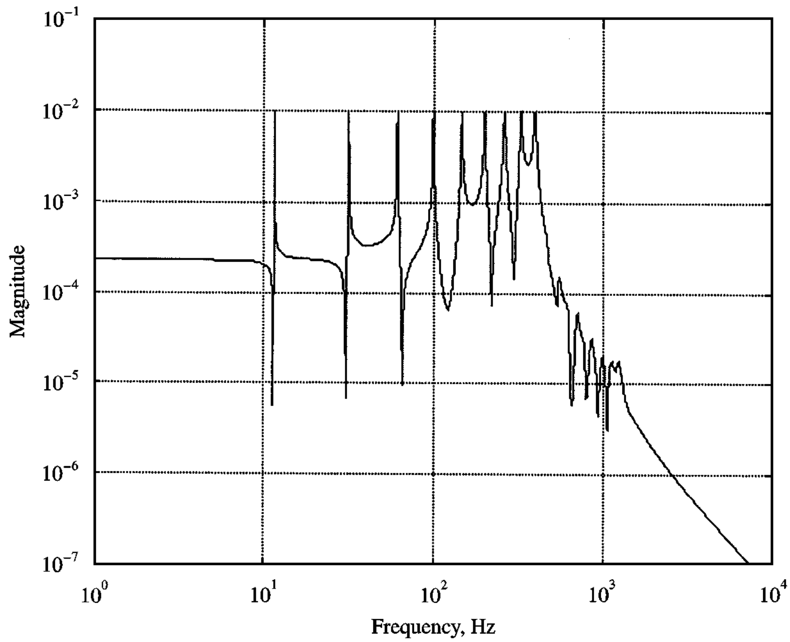

Figure 7. Magnitude of a transfer function for the nine-mode modal actuator.

do not follow any particular mode shape. The width of a piezoelectric actuator that corresponds to the input matrix B_o and excites all nine modes is shown in Figure 6.

The plot of the transfer function of the single-input system with the input matrix B_o is shown in Figure 7. The plot shows that all the nine modes are excited, with approximately the same amplitude of 0·01 cm. Figure 5(a) shows the impulse response at node 6. The time history consists of nine equally excited modes. Figure 5(b) shows the simultaneous displacement in y direction of all nodes. The rather chaotic pattern of displacement indicates the presence of all nine modes in the response.

4. MODAL SENSORS

The modal sensor determination is similar to the determination of modal actuators. The governing equation is derived from equation (4). If one wants to observe a single mode only (say ith mode) one assumes the modal output matrix in the form $C_{mq} = [0 \quad \cdots \quad 0 \quad 1 \quad 0 \quad \cdots \quad 0]$, where 1 stands at the ith position. The corresponding output matrix is obtained from equation (4),

$$C_{oq} = C_{mq}\Phi^{+}, \tag{11a}$$

where Φ^{+} is the pseudoinverse of Φ. Similarly, one obtains the rate sensor matrix C_{ov} for the assigned modal rate sensor matrix C_{mv},

$$C_{ov} = C_{mv}\Phi^{+}. \tag{11b}$$

Above we assumed that the assigned modes are observable, i.e., that the rank of Φ is n_m, where n_m is the number of the assigned modes.

Multiple modes with assigned amplitudes are obtained using sensor weights. The weighted sensors are obtained from equation (8). Namely, the ith weight is determined from

$$w_i = \frac{2\zeta_i\omega_i\|G_i\|_\infty}{\|b_{mi}\|_2}, \tag{12}$$

where $\|G_i\|_\infty$ is the amplitude of the ith mode.

4.1. EXAMPLE 3

The beam from Figure 1 with three vertical force actuators located at nodes 2, 7, and 12 is considered. Find the displacement output matrix C_{oq} such that the first nine modes have equal contribution to the measured output with amplitude 0·01.

The matrix C_{mq} that excites first nine modes is the unit matrix of dimension 9 of gain 0·01, i.e., $C_{mq} = 0{\cdot}01 \times W \times I_9$. The weights W that make the mode amplitudes approximately equal were determined from equation (12). The output matrix C_{oq} is determined from equation (11). For this matrix the magnitudes of the transfer functions of the nine outputs in Figure 8 show that all nine of them have a resonance peak of 0·01.

4.2. EXAMPLE 4

The beam from Figure 1 with actuators as in Example 3 is considered. Find the nodal rate sensor matrix C_{ov} such that all nine modes but mode 2 contribute equally to the measured output with the amplitude of 0·01.

The matrix C_{mv} that gives in the equal resonant amplitudes of 0·01 is $C_{mv} = 0{\cdot}01 \times W \times [1 \quad 0 \quad 1 \quad 1 \quad 1 \quad 1 \quad 1 \quad 1 \quad 1]$, where the weight W is determined from

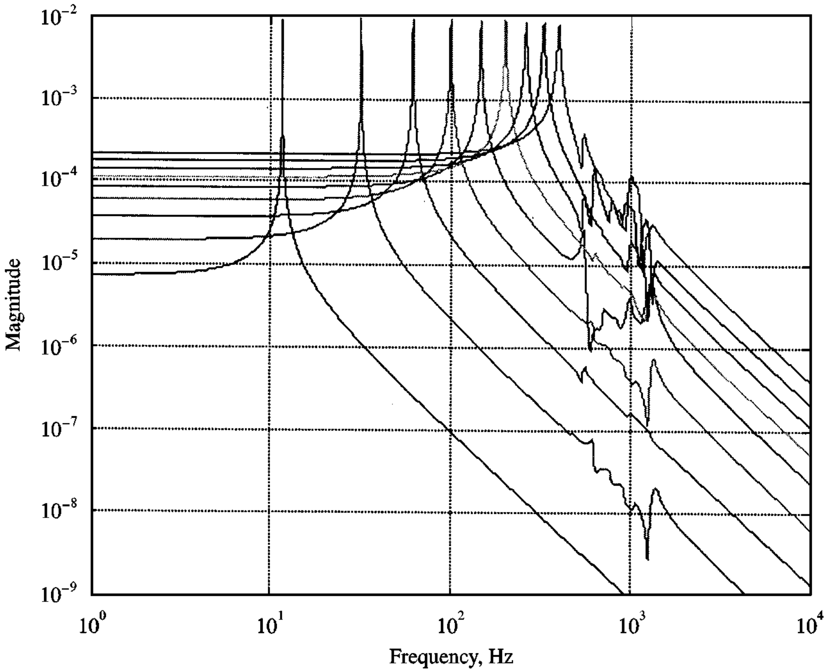

Figure 8. Magnitude of the transfer function with the nine single-mode sensors for the first nine modes.

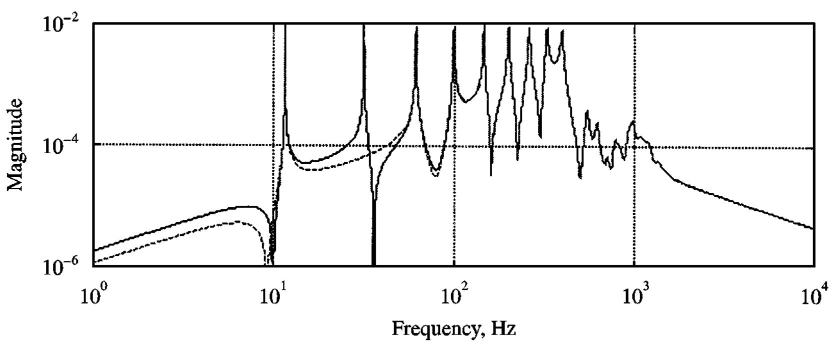

Figure 9. Magnitude of the transfer function with the nine-mode sensor (solid line), and for the eight-mode sensor (dashed line). The latter includes the first nine modes but the second one.

equation (12), and the output matrix C_{ov} is obtained from equation (11b). For this matrix the magnitude of the transfer function is shown in Figure 9, dashed line. It is compared with the magnitude of the transfer function for the output that contains all the nine modes (solid line). It is easy to notice that the second resonance peak is missing in the plot.

REFERENCES

1. W. H. Ko 1996 *Sensors and Actuators A* **56**, 193. The future of sensor and actuator systems.

2. W. Gawronski 1998 *Dynamics and Control of Structures: A Modal Approach*. New York: Springer.
3. W. Gawronski and K. B. Lim 1996 *International Journal of Control* **65**, 131. Balanced actuator and sensor placement for flexible structures.
4. M. L. Delorenzo 1990 *Journal of Guidance, Control and Dynamics* **13**, 249. Sensor and actuator selection for large space structure control.
5. K. B. Lim 1992 *Journal of Guidance, Control and Dynamics* **15**, 49. Method for optimal actuator and sensor placement for large flexible structures.
6. K. B. Lim and W. Gawronski 1993 *Control and Dynamics Systems*, Vol. 57 (C. T. Leondes, editor) 109. San Diego: Academic Press. Actuator and sensor placement for control of flexible structures.
7. P. G. Maghami and S. M. Joshi 1990 *IEEE American Control Conference, San Diego, CA*, 1941. Sensor/actuator placement for flexible space structures.
8. M. Salama, T. Rose and J. Garba 1987 *28th Structures, Structural Dynamics and Materials Conference, Monterey, CA*, 1024. Optimal placement of excitations and sensors for verification of large dynamical systems.
9. A. Hac and L. Liu 1993 *Journal of Sound and Vibration* **167**, 239. Sensor and actuator location in motion control of flexible structures.
10. K. B. Lim 1997 *Journal of Guidance, Control and Dynamics* **20**, 202. Disturbance rejection approach to actuator and sensor placement.
11. W. Gawronski 1997 *Journal of Sound and Vibration* **208**, 101. Actuator and sensor placement for structural testing and control.
12. A. W. Phillips and R. J. Allemang 1996 *Proceedings of 14th International Modal Analysis Conference, Deaborn, MI*, 253. Single degree-of-freedom modal parameter estimation methods.
13. N. M. M. Maia and J. M. M. Silva (editors) 1997 *Theoretical and Experimental Modal Analysis*. Taunton, England: Research Studies Press Ltd.
14. J. E. Cooper and J. R. Wright 1997 *Proceedings of 15th International Modal Analysis Conference, Orlando, FL* 1353. To fit or to tune? That is the question.
15. C.-K. Lee and F. C. Moon 1990 *Journal of Applied Mechanics, Transactions of ASME* **57**, 434. Modal sensors/actuators.
16. C.-Y. Hsu, C.-C. Lin and L. Gaul 1998 *Smart Materials and Structures* **7**, 446. Vibration and sound radiation controls of beams using layered modal sensors and actuators.
17. S. O. Oyadiji and M. Solook 1997 *Smart Sensing, Processing, and Instrumentation, Proceedings of SPIE* **3042**, 24. Selective modal sensing of vibrating beams using piezoelectric beams.
18. W. Gawronski 1996 *Balanced Control of Flexible Structures*. London: Springer.